

Discrete atomistic model to simulate etching of a crystalline solid

Bernardo A. Mello*

Physics Department, Catholic University of Brasília, 72030-170, Brasília-DF, Brazil

Alaor S. Chaves and Fernando A. Oliveira

Institute of Physics and International Centre of Condensed Matter Physics, University of Brasília, Caixa Postal 04513, 70919-970, Brasília-DF, Brazil

(Received 15 November 2000; published 28 March 2001)

A discrete atomistic solid-on-solid model is proposed to describe dissolution of a crystalline solid by a liquid. The model is based on the simple assumption that the probability per unit time of a unit cell being removed is proportional to its exposed area. Numerical simulations in one dimension demonstrate that the model has very good scaling properties. After removal of only about 10^2 monolayers, independently of the substrate size, the etched surface shows almost time-independent short-range correlations and the receding surface presents the Family-Vicsek scaling behavior. The scaling parameters $\alpha = 0.491 \pm 0.002$ and $\beta = 0.330 \pm 0.001$ indicate that the system belongs to the Kardar-Parisi-Zhang universality class. The imposition of periodic boundary conditions on the simulations reduces the effective system size by a factor of 0.68 without changing the exponents α and β . Surprisingly, the periodic condition changes drastically the statistics of the surface height fluctuations and the short-range correlations. Without periodic conditions, that statistics is, up to 3 standard deviations, an asymmetric Lévy distribution with $\mu = 1.82 \pm 0.01$, and outside this region the statistics is Gaussian. With periodic conditions, that statistics is Gaussian, except for large negative fluctuations.

DOI: 10.1103/PhysRevE.63.041113

PACS number(s): 05.40.Fb, 05.45.Df, 68.35.Ct, 68.08.-p

I. INTRODUCTION

In the last 15 years there has been intensive research on far from equilibrium moving surfaces [1–3]. Those surfaces can be related to expanding fire, fluid flowing in a porous media, growing bacteria colonies, growth of colloidal aggregates, epitaxial growth of crystalline solids on a flat substrate, or etching of a crystalline solid by a liquid, a gas, a plasma, or a beam of atomic ions (sputtering), and others. It is well established that many of those moving surfaces have self-affine morphologies with simple space and time scaling properties. The morphology of the surface is more easily described in the case of epitaxial growth on an initially flat horizontal substrate of dimensionality d and linear dimension L . The vertical position of the grown film surface at the horizontal coordinate \mathbf{r} , elapsed a time t after the growth start, is $h(\mathbf{r}, t)$. The roughness of the surface is measured by the rms deviation of the surface height, $w(L, t) = \langle [h(\mathbf{r}, t) - \bar{h}(t)]^2 \rangle^{1/2}$, where $\bar{h}(t)$ is the average film thickness. For a large class of growing systems, the roughness kinetics satisfy the Family-Vicsek scaling ansatz [4]

$$w(L, t) = L^\alpha f(t/L^{\alpha/\beta}), \quad (1)$$

where the function $f(u)$ has the limiting behavior $f(u) \sim u^\beta$ for $u \ll 1$ and $f(u) = \text{constant}$ for $u \gg 1$. Therefore, for $t \ll t_\times = C_{t_\times} L^{\alpha/\beta}$, $w = C_w t^\beta$, and for $t \gg t_\times$, $w_s = C_{w_s} L^\alpha$, where the subscript s in w stands for saturated.

Theoretically, the growth kinetics has been widely described by continuum Langevin equations of the type

$$\begin{aligned} \frac{\partial h}{\partial t} = & \nu \nabla^2 h + \lambda (\nabla h)^2 + \dots + \nu_n \nabla^{2n} h + \kappa (\nabla^2 h) (\nabla h)^2 \\ & + \dots + \kappa_{kj} (\nabla^{2k} h) (\nabla h)^{2j} + F + \eta(\mathbf{r}, t), \end{aligned} \quad (2)$$

where n , k , and j are positive integers, F is the average particle flux on the substrate, and $\eta(\mathbf{r}, t)$ is an uncorrelated noise. This family of equations leads to the scaling expressed by Eq. (1), and the exponents α and β depend on the coefficients ν , λ , ν_n , κ , and κ_{kj} , which have a nonzero value; the F and η terms are of course always present. Thus, each equation of the family defines one universality class of moving surfaces, each family presenting well-defined values for α and β . The most important universality classes are defined by the Edwards-Wilkinson (EW) equation [5], which contains only the $\nabla^2 h$ surface tension term in Eq. (2), and the Kardar-Parisi-Zhang (KPZ) equation [6] which also contains the nonlinear term $(\nabla h)^2$.

A very large number of discrete atomistic models for numerical simulation of the moving surfaces has also been proposed, and many of them demonstrated to present the Family-Vicsek scaling. Some of these are very simple models intended not to describe in detail any specific system, but to demonstrate on a microscopic basis the generation of a self-affine moving surface. The most widely investigated atomistic models are the ballistic deposition (BD) [7] and extensions of the random deposition model, which allow particle diffusion, as for example the Wolf-Villain (WV) model [8] (for reviews, see [1,2]). Those models present some characteristics that limit their usefulness in the investigation of surface morphology. The BD model generates films with vacancies and overhangs that create difficulties for the analysis of the film; not only the film surface but also its body are fractal systems, and it is also difficult to define univocally the

*Electronic addresses: bernardo@icomp.br, fao@icomp.br, alaor@icomp.br

film surface. The WV model belongs to the solid-on-solid models free from vacancies and overhangs. However, it is known [9,10] that the generated films present anomalous scaling, in the sense that before the deposition of rather thick films [up to 10^6 monolayers (ML) for the $d=1$ case], the system does not satisfy the scaling law given by Eq. (1). Thus, calculation of the correct α and β scaling exponents requires simulation with very large substrates and the growth of thick films.

In this paper we propose a simple atomistic model for dissolution that mimics the etching of a crystalline solid by a liquid. The numerical simulations for the $d=1$ dimensionality indicate that the model belongs to the KPZ universality class. The calculations demonstrate that the model presents exceptionally good scaling properties. After a transient of only about 20 dissolved monolayers, independently of the substrate size L , the receding surface satisfies the Family-Vicsek scaling, and hence the scaling properties and the correct scaling exponents can be obtained from calculations on rather small substrates.

We also investigated the statistics of the surface height fluctuations, expressed by $P(\Delta h_i)$, where Δh_i is the difference between the height at site i and the average height $\bar{h}(t)$. For $t \ll t_\times = C t_\times L^{\alpha/\beta}$, $P(\Delta h_i)$ is a Gaussian distribution. However, the statistics present a crossover at $t = t_\times$. For $t \gg t_\times$, $P(\Delta h_i)$ can be fitted, within the accuracy of the data, by an asymmetric Lévy distribution in the rather wide range $|\Delta h_i| < 3w_s$ and is approximately a Gaussian outside that range of fluctuations. We argue in this paper that this asymmetry in the surface fluctuation should be true for any model belonging to the KPZ universality class, as well as other classes in which nonlinear terms like $(\nabla h)^{2j}$ appear in Eq. (2).

The investigation of $P(\Delta h_i)$ also uncovered the as yet unnoticed fact that the morphology of the surface is sensitive to the boundary conditions in quite a surprising way: for surfaces simulated using periodic boundary conditions (PBC) $P(\Delta h_i)$ is quite precisely a Gaussian distribution, except for large negative values of Δh_i . As there is no physical reason for imposing PBC on the simulation, we consider as valid the results obtained with nonperiodic boundary conditions (NBC).

II. MODEL AND SIMULATION

The substrate is a square lattice with a one-dimensional surface exposed to dissolution. The model states that the probability per unit time of a unit cell being removed is proportional to its number of free sides. This can be justified by the fact that the number of collisions per unit time that the solvent molecules make with one cell is proportional to its exposed area. It is also supposed that the solution remains sufficiently diluted and hence readsorption is ignored. It must be recognized that the model cannot accurately describe wet etching because it ignores the fact that the energy necessary to remove a cell also depends on the number of free sides.

Another model for crystal dissolution had been proposed [11] in which the probability per unit time of a cell being removed is proportional to $\exp(-nw)$, where n is the number

of the cell's nearest neighbors and w is a model parameter. This model emphasizes the dependence of the binding energy of the cell with the number of nearest neighbors. The referred model changes its universality class as the parameter w varies and also present overhangs. A physically more realistic model would be a combination of these two. However that hypothetical model would present the complicated scaling properties arising from the $\exp(-nw)$ dependence. At the present stage of the investigation of growth dissolution processes the emphasis still is on models with simple scaling properties, in order to understand the most general laws governing those processes.

The cellular automata algorithm that simulates this model is

(1) select randomly one horizontal site $i=1,2,\dots,L$ at discrete instant T ;

(2) $h_i(T+1) = h_i(T) + 1$;

(3) if $h_{i-1}(T) < h_i(T)$ do $h_{i-1}(T+1) = h_i(T)$;

(4) if $h_{i+1}(T) < h_i(T)$ do $h_{i+1}(T+1) = h_i(T)$.

When PBC is not imposed, i.e., in the case of NBC, the existence of the external (vertical) exposed faces of the cells at the borders is ignored. In this case, step 3 is not executed when $i=1$ and step 4 is not executed when $i=L$. Therefore, the system acts as if the end vertical surfaces of the substrate were covered with a protection to avoid lateral etching. It must be noticed that the substrate is etched upwards, which makes easier the analogy with the more widely studied growth kinetics.

Calculations were performed up to $t=20t_\times$, where $t = T/L$, which means deep inside the saturation regime, for substrate sizes $L = 128, 256, 512, 1024, 2048, 4096$, and 8192 . Satisfactory data on the tails of the distributions $P(\Delta h_i)$ were obtained by performing simulations over, respectively, 1×10^6 , 1.2×10^6 , 2.6×10^5 , 7.1×10^4 , 1.6×10^4 , 3.7×10^3 , and 9×10^2 substrates for PBC and 3.9×10^6 , 1.5×10^6 , 3.2×10^5 , 7.1×10^4 , 2×10^4 , 3.4×10^3 , and 9×10^2 substrates for NBC. Calculations were also performed on a large substrate with dimension $L=131072$, in the regime $t \ll t_\times$, to obtain a more precise determination of the exponent β . We used a long period ($> 2 \times 10^{18}$) random number generator of L'Ecuyer with Bays-Durham shuffle and added safeguards (*ran2* of Ref. [12]).

III. SHORT-RANGE CORRELATIONS

Figure 1(a) shows the time evolution of the average step size $a(t) = \langle |h_i(t) - h_{i-1}(t)| \rangle$ and the rms step size $a_{\text{rms}}(t) = \langle [h_i(t) - h_{i-1}(t)]^2 \rangle^{1/2}$, for simulations with PBC and several substrate sizes. The figure shows that both $a(t)$ and $a_{\text{rms}}(t)$ are almost independent of the substrate size and that after $t \approx 10^2$ those two functions saturate at constant values. This means that the surface fluctuations quickly builds up short-range correlations that remain unchanged while progressively the correlation length grows up with time until becoming equal to L . This behavior is considered important for the quick establishment of the Family-Vicsek scaling law [9–11,13]. The average step size works as a natural unit for the surface height fluctuations, and after $a(t)$ saturates at a constant value, the function $h(r,t)$ is expected to satisfy a

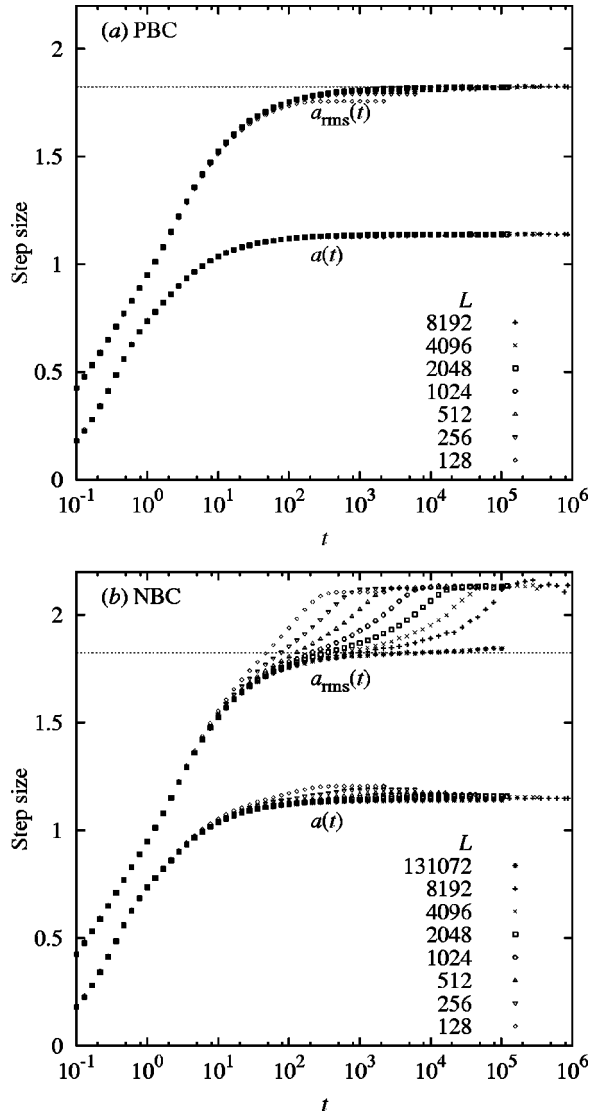


FIG. 1. Step size measured by $a(t)$ and $a_{\text{rms}}(t)$ for simulations with (a) periodic boundary conditions and (b) nonperiodic boundary conditions. The horizontal dotted line is the saturation value (1.826 ± 0.001) of a_{rms} for simulations with periodic boundary condition.

dynamical equation like Eq. (2) in which the coefficients ν , λ , ν_n , etc., are time independent. For comparison, in the WV model, $a_{\text{rms}}(t)$ depends on the substrate size and for $L > 200$ that step size remains increasing until $t \geq 10^6$ [9].

Figure 1(b) shows the same time evolution of the step sizes shown in Fig. 1(a), but for calculations with NBC. One sees that the time evolution of $a(t)$ is almost the same for both kinds of boundary conditions. However, now the evolution of $a_{\text{rms}}(t)$ shows a distinct behavior. Its saturation value is 16% higher than in the case of PBC, and besides the saturation only occurs at later times. In fact, for large substrates, one can observe that $a_{\text{rms}}(t)$ presents a pseudosaturation at the same value observed for simulations with PBC, indicated in the figure by a dotted line, at the same time $t \approx 10^2$, and later on gains a new step. As will be seen in Sec. V, the change of $a_{\text{rms}}(t)$ from the dotted line level to a higher

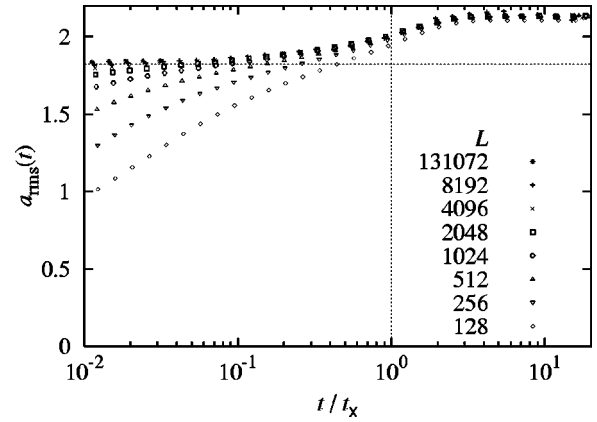


FIG. 2. The $a_{\text{rms}}(t)$ step size of Fig. 1(b) expressed as function of the reduced time t/t_{\times} . The figure shows that the crossover from the pseudosaturation value of $a_{\text{rms}}(t)$ to the true saturation value occurs at t_{\times} .

value is related to a change in the statistics of the surface height fluctuation, which is initially Gaussian and later on becomes of Lévy type. The true saturation of $a_{\text{rms}}(t)$ only occurs at $t = t_{\times}$, obtained as described in the next section. This indicates that the absence of PBC allows some large and rare big steps that affects the value of $a_{\text{rms}}(t)$ but have little influence on $a(t)$, which is a signature of the Lévy distribution of surface height fluctuations. Figure 2 shows the same data of Fig. 1(b) as a function of the reduced time t/t_{\times} , to show explicitly that $a_{\text{rms}}(t)$ only saturates at $t = t_{\times}$.

It is usually accepted that the Family-Vicsek behavior occurs only after the short-range correlation has been established. However this is not true, as can be seen by comparing Fig. 1(b) and Fig. 3(a). Those figures show that the Family-Vicsek behavior starts when the step size reaches the pseudosaturation value. This happens because the transition from the pseudosaturation value to saturation value occurs at the same crossover time t_{\times} that governs the global behavior. The boundary-condition influence in the small range correlation is an unexpected result.

IV. SCALING LAWS

Figures 3(a) and 3(b) show in log-log plots the time evolution of the surface roughness $w(L, t)$ for simulations with NBC and PBC, respectively. A careful examination of those figures shows that PBC results in earlier roughness saturation, as compared to NBC. This occurs because the imposition of PBC is in some sense equivalent to a reduction of the substrate size L . This can be clearly observed by comparison of Figs. 3(a) and 3(b). The figures also show that the scaling behavior $w(L, t) = C_w t^{\beta}$ only applies for $t > 10$ (etching of about 20 ML). For a more precise determination of β , only the data of the $L = 131\,072$ substrate were considered and the obtained value was 0.330 ± 0.001 . Figure 4 shows in a log-log plot the time evolution of the reduced width $w(L, t)/w_s$ with the reduced time t/t_{\times} , for simulations with NBC.

Figure 5 shows in a log-log plot the variation with the substrate size of the saturated roughness, for simulations using both PBC and NBC. The exponent α was calculated

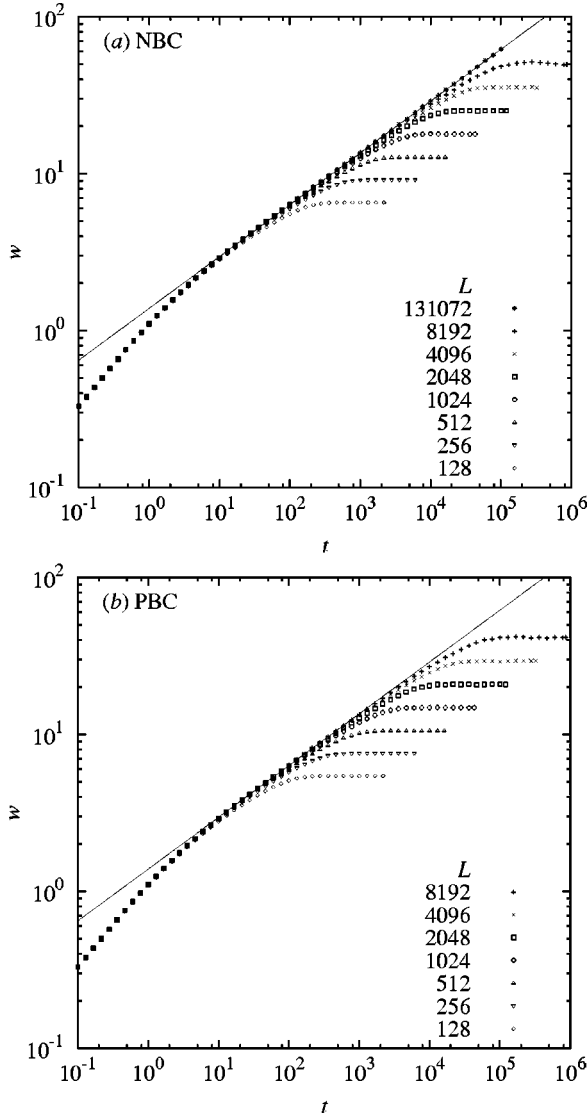


FIG. 3. (a) Time dependence of the roughness of substrates with nonperiodic boundary conditions. The straight line is the roughness growth law obtained from the 131 072 substrate between time 10^3 and 10^5 . The power law is $(1.384 \pm 0.008)t^{0.330 \pm 0.001}$. (b) Same as (a) for periodic boundary conditions.

from the slope of both curves in Fig. 5, using only the substrates with L larger than 1000, with the results $\alpha = 0.4961 \pm 0.0003$ for PBC and $\alpha = 0.491 \pm 0.002$ for NBC. We point out that the obtained values of α and β are very close to those calculated for the $d=1$ KPZ equation, namely, $\alpha = 1/2$ and $\beta = 1/3$. In fact, to our knowledge, this is the best agreement with the KPZ equation ever obtained from an atomic discrete model. This indicates that the present model for wet etching belongs to the KPZ universality class. Figure 5 shows with more clarity the fact previously noticed that the imposition of PBC implies the reduction of the effective substrate size, as the two straight lines have almost the same slope and therefore can be brought to coincidence (superposition) by a vertical translation. More explicitly, the line corresponding to simulation with NBC will coincide with that corresponding to simulation with PBC if the corresponding

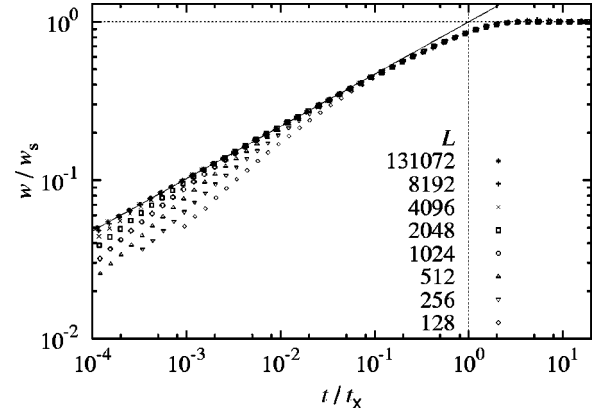


FIG. 4. Universality curves obtained by renormalizing Fig. 3(a).

values of w_s are multiplied by 0.829. This is equivalent to reducing the substrate size in simulations with PBC: $L_{\text{PBC}} = 0.829^{\alpha/\beta} L_{\text{NBC}} = 0.68 L_{\text{NBC}}$. Our calculations with the data of Fig. 3(a) and 3(b) also show that the crossover time $t_{\times} = C_{t_{\times}} L^{\alpha/\beta}$ is reduced by a factor of 0.567 when the PBC is imposed. Hence, we should expect that the imposition of PBC implies a reduction of L by a factor of 0.68, in very good agreement with the factor of 0.68 previously obtained.

Figure 6 shows in a log-log plot the structure factor

$$S(k, t) = \langle \tilde{h}(k, t) \tilde{h}(-k, t) \rangle, \quad (3)$$

where

$$\tilde{h}(k, t) = L^{-1/2} \sum_{j=1}^L [h_j(t) - \bar{h}(t)] e^{i(jk)}, \quad (4)$$

for $t \gg t_{\times}$, and simulations with NBC. It is known [10] that, for this saturated regime,

$$S(k, t) \propto k^{-2\alpha-d}. \quad (5)$$

However, for discrete systems with unit-cell size a , this relation cannot be valid for wave vectors close to the Brill-

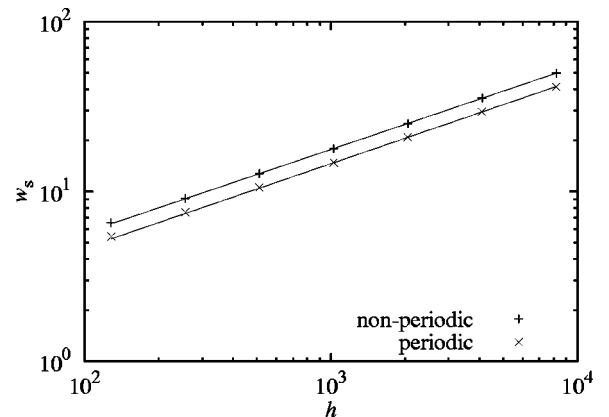


FIG. 5. Length dependence of saturated roughness. The power law was obtained from the substrates larger than 10^3 . For periodic conditions it is $(0.4740 \pm 0.0013)L^{0.4961 \pm 0.0003}$, and for nonperiodic it is $(0.594 \pm 0.008)L^{0.491 \pm 0.002}$.

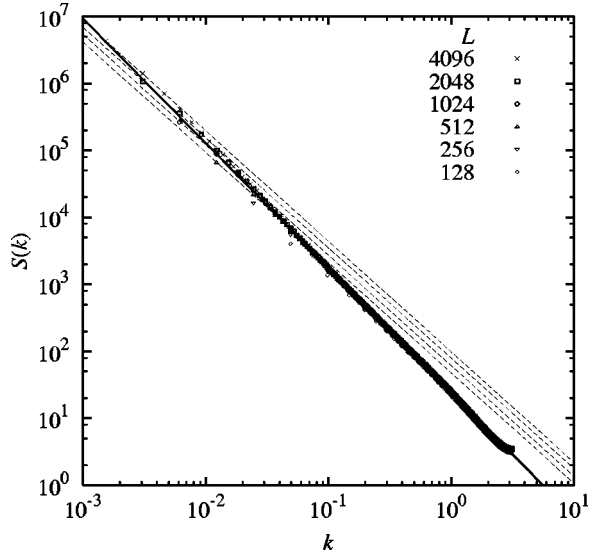


FIG. 6. Structure factor for different substrates, for simulations with NBC. The results for simulations with PBC are visually not very different. The solid line is a power law with exponents -1.92 ± 0.02 , fitted in the range $0.05 \leq k \leq 0.1$. The dashed lines have exponents -1.65 ± 0.05 and was fitted to the three first points of each curve, the upper for $L=4096$.

lounin zone boundary $k_{ZB} = \pi/a$, in the present case $k_{ZB} = \pi$. In fact, $\partial S(k,t)/\partial k|_{k=\pi} = 0$, as can be observed in Fig. 6. The dashed lines in the figure are linear fittings of the three smallest wave vectors of each curve. All these straight lines have the same slope $-\gamma' = -1.65 \pm 0.05$. Comparing this with Eq. (5) for the case $d=1$, we obtain $\alpha = 0.325 \pm 0.025$, in clear disagreement with the value of α obtained from the scaling law $w_s = C w_s L^\alpha$. The solid line in Fig. 6 is a fit of the intermediate region of the curve, ignoring the bending both at small values of k and very close to k_{ZB} . Its slope is $-\gamma = -1.92 \pm 0.02$. With this value of γ we obtain $\alpha = 0.46 \pm 0.01$, in reasonable agreement with the value $\alpha = 0.491 \pm 0.002$ obtained from the Family-Vicsek scaling law. This confirms that for finite and discrete systems, the law expressed by Eq. (5) fails both for very small k and for k close to the zone boundary. The deviation for small k is really a small-size effect, as can be seen from the examination of the figure; the larger the substrate, the smaller the value of k for which the curve deviates from the solid straight line. The reasonable agreement between the values of α determined by those two distinct methods is an independent indication that the present model does not present anomalous scaling [10].

V. STATISTICS OF THE SURFACE HEIGHT FLUCTUATIONS

As compared to the very intensive investigation of the scaling behavior of the moving surface, there has been very little study of the fluctuations of the surface height. In fact, the existing studies were motivated by experiments demonstrating very large values of α and β . Experiments on fluid flow in porous media [14] give $\alpha \approx 0.81$ and $\beta \approx 0.625$, and

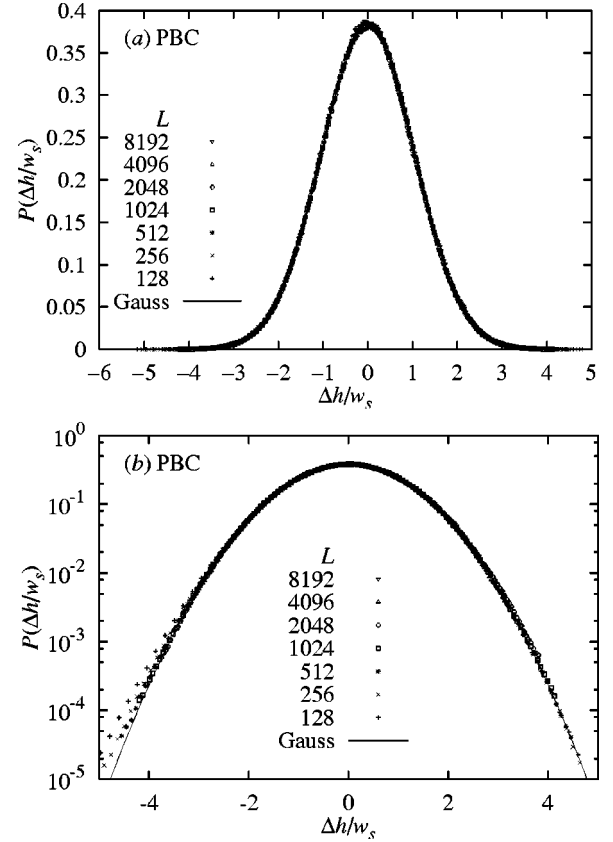


FIG. 7. (a) Distribution of the saturated surface height fluctuation expressed in reduced substrate-size-independent units, for simulations with periodic conditions. (b) Same data of (a) in a semilog plot. The Gaussian distribution is obeyed in the whole range of height fluctuations. However the probability of large negative fluctuations is clearly larger than the predictions of Gaussian distribution.

from these values one obtains $\alpha + \alpha/\beta \approx 2.1$, which indicate that the system belongs to the KPZ universality class, in which holds the relation $\alpha + \alpha/\beta = 2$. Zhang [15] suggested that the large values of α and β can be explained by an uncorrelated noise obeying a power-law probability distribution $P(\eta) \sim \eta^{1-\zeta}$, where $\eta \geq 1$. Both numerical simulations and analytical results [15–17] gave support to this proposal. For $d=1$ films, the calculated values of the scaling exponents are [17] $\alpha = 3/(\zeta + 1)$, $\beta = 3/(2\zeta - 1)$, ($\zeta > 2$), and $\alpha = \beta = 2/\zeta$, ($\zeta < 2$).

We made extensive analysis of the probability distribution of the surface height fluctuations for the saturated regime $t \gg t_\infty$. One important conclusion is that $P(\Delta h_i)$ is sensitive to the boundary conditions. Figure 7(a) and 7(b) shows, in linear and semilog plots, respectively, $P[\Delta h/w_s(L)]$ as a function of $\Delta h/w_s(L)$ (note that the subscript i in h_i was omitted) in the saturated regime for the simulation with PBC. The distributions for all sample sizes fall onto the same universal curve that can be fitted quite precisely with a Gaussian, except for large negative Δh . Figures 8(a) and 8(b) show the same as Figs. 7(a) and 7(b) for samples simulated with NBC. It is immediately clear that, in contrast with what happens with the samples simulated with PBC, now the sur-

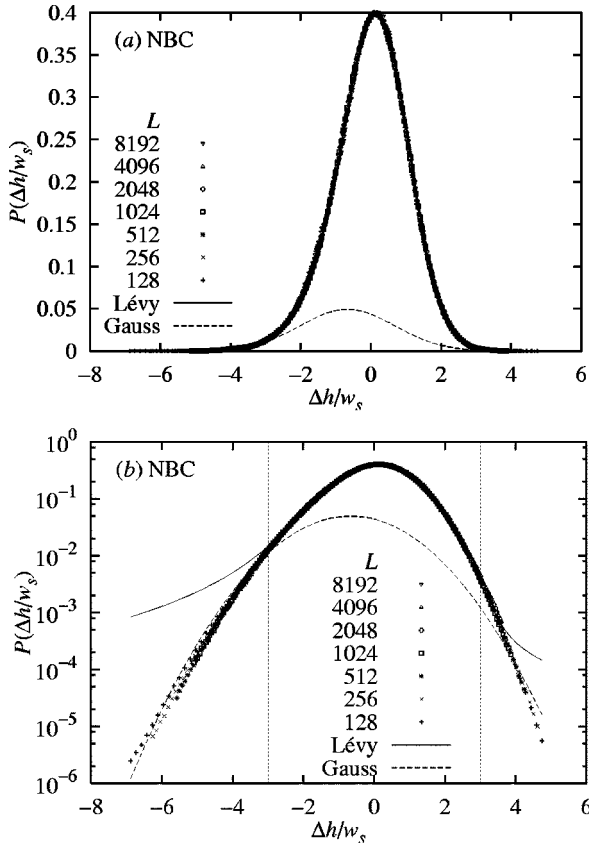


FIG. 8. (a) Distribution of the saturated surface height fluctuation expressed in reduced substrate-size-independent units, for simulations without periodic conditions. (b) Same data of (a) in a semilog plot. The height fluctuations follow an asymmetric Lévy distribution for $|\Delta h/w_s| < 3$, and an approximately Gaussian distribution outside this range. The parameters of the Lévy distribution are $\mu = 1.82 \pm 0.01$ and $\xi = -0.80 \pm 0.05$.

face height distributions fall onto the same universal asymmetric curve. That asymmetry demonstrates that the height fluctuations do not follow a Gaussian distribution. That is a main result of this paper and will be discussed in some detail.

Recently [18], it was shown that a fractional diffusion equation (involving fractional derivatives $\partial_x^\mu \equiv \partial^\mu / \partial x^\mu$, μ fractionary) in an asymmetric medium, $\partial n / \partial t = (D_l \partial_x^\mu + D_r \partial_{-x}^\mu) n / 2$, leads to a particle distribution, which in one dimension is expressed by

$$P(x, t) = \int_{-\infty}^{\infty} \frac{1}{2\pi} p(k, t) e^{ikx} dk, \quad (6)$$

where the characteristic function is

$$p(k, t) = \exp \left[\frac{|k|^\mu}{2} (D_l + D_r) \cos \left(\mu \frac{\pi}{2} \right) t \right] \times \exp \left[ik \frac{|k|^{\mu-1}}{2} (D_l - D_r) \sin \left(\mu \frac{\pi}{2} \right) t \right], \quad (7)$$

with $1 < \mu < 2$. This is an asymmetric Lévy distribution.

As the fractional diffusion equation just described is predicted to hold in a fractal system, and that is the case of the moving etched surface, we speculate that it can describe the evolution of the stochastic variable $\Delta h_i(t)$ in the continuum limit. The time variable that appears in Eqs. (6) and (7) obviously does not have any meaning in the analysis of the surface height fluctuation for $t \gg t_\times$. Hence, we tried to fit the distributions shown in Figs. 8(a) and 8(b) with the asymmetric Lévy distribution

$$P(x) = \frac{A}{\pi} \int_0^\infty \cos[k(x - x_0) + C \xi k^\mu \tan(\mu \pi / 2)] \times \exp(-Ck^\mu) dk, \quad (8)$$

where $\xi = (D_l - D_r) / (D_l + D_r)$ and $x = \Delta h / w_s$. Figure 8(a) shows the result of this fitting for the data plotted in linear scales. The fitting curve is a solid line completely covered by the simulated data, which suggests a very good fitting. However, when the same data are exposed in a semilog plot, as shown in Fig. 8(b), it becomes clear that the Lévy distribution deviates from the data outside the region $|\Delta h/w_s| > 3$. The dashed lines shown in both Figs. 8(a) and 8(b) are the best fit using a Gaussian. One can see that the distant tails of the data distribution can be approximately fitted by a Gaussian distribution. In fact, in order to have really good agreement, we had to use two distinct Gauss functions, one for each tail, but this fitting is not shown and is not relevant in our analysis. We conclude that the not-too-large (up to three standard deviations w_s) surface fluctuations can be described, within the accuracy of the data, by an asymmetric Lévy distribution, whereas the very large surface fluctuations follow a Gaussian distribution. The fitting parameters of the Lévy distribution are $\mu = 1.82 \pm 0.01$ and $\xi = 0.80 \pm 0.05$.

Figures 9(a) and 9(b) show, respectively, the time evolution of the parameters μ and ξ as the etching progresses. At the beginning, $\mu \approx 2$, which means that the surface fluctuations are Gaussian. This explains why the values of $a_{\text{rms}}(t)$ have the same behavior at early times for both PBC and NBC, as can be seen comparing Figs. 1(a) and 1(b). For μ very close to 2, the Lévy distribution is almost insensitive to the value of ξ , and consequently the values of this asymmetry parameter at early times are very imprecise.

We argue that, for any moving active surface belonging to the KPZ universality class, the surface height fluctuations must have an asymmetric distribution. In fact, owing to the nonlinear $\lambda(\nabla h)^2$ term in Eq. (2), the symmetry of the surface under the transformation $h \rightarrow -h$ is broken. This means that the positive ($\Delta h > 0$) and negative ($\Delta h < 0$) fluctuations of the surface height are statistically different. If $\lambda = 0$, that surface symmetry is recovered; hence, the positive and negative fluctuations of the surface height become statistically equivalent, and the distribution $P(\Delta h/w_s)$ is expected to become symmetric, either by a symmetric Lévy distribution ($D_l = D_r$) or a Gaussian. On passing, it is opportune to remark that the Gaussian and Lévy distributions are the only invariants of the renormalization-group transformation of the random-walk distributions [19]. Thus, we conclude that the moving surfaces belonging to the EW universality class must

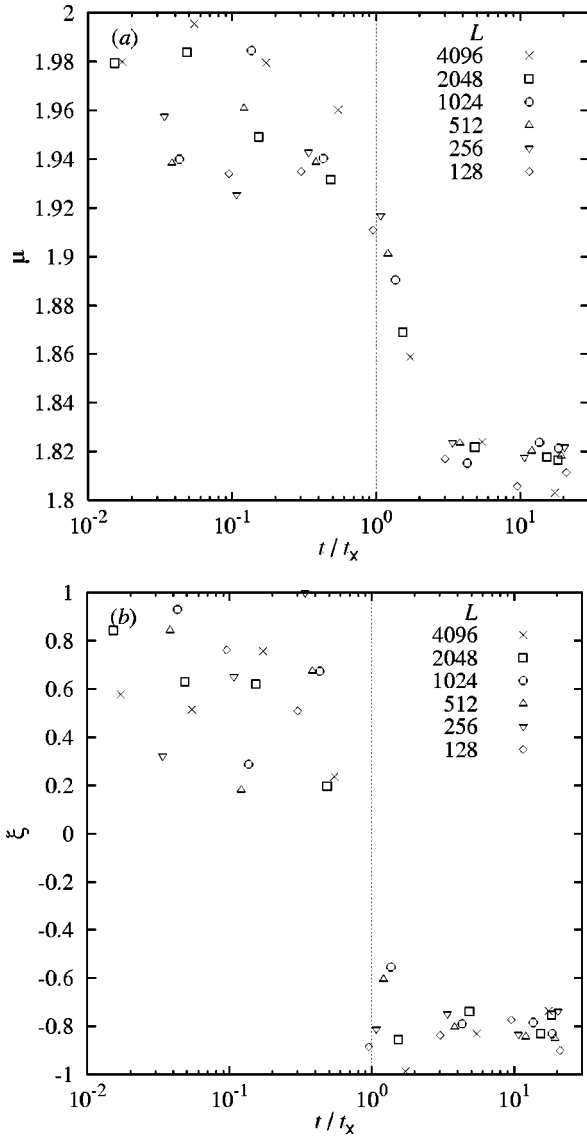


FIG. 9. Time evolution of (a) the μ exponent and (b) the asymmetry parameter ξ of the Lévy distribution that fits the central part of the surface height fluctuation.

show symmetric distribution of heights fluctuation. Physically, it seems that symmetric surfaces, in which the hills are statistically similar to the valleys, can be obtained only under very special conditions of growth or erosion. One example of a very asymmetric surface is that obtained by polishing a solid with grinding powder: the polished surface presents valleys caused by scratches but not the analogous hills. The nonlinear term $(\nabla h)^2$ in the KPZ equation is what distinguishes hills from valleys and is essential to describe all those asymmetric moving surfaces.

We now address the change of the statistics of the surface fluctuations for very large fluctuations. The first point to remark is that though the Lévy distributions are very common in nature (for reviews, see [20,21]), including the distribution of step lengths in diffusive processes, studies of the density distributions of particles performing anomalous diffusion are very rare. Usually, only measurements of the variance of the particles positions are reported, not the particle density dis-

tributions. To our knowledge, the only exception is the study of diffusion of a photoexcited electron-hole plasma in a semiconductor quantum well [22]. That paper shows that the particle density obeys a Lévy distribution with $\mu=1.3$. The asymmetry parameter is $\xi=0$ or $\xi \approx -1$ depending on whether the quantum well is aligned or slightly tilted relative to the crystallographic axes. One clear point is that, as the measured particles variance must be finite and the Lévy distribution has an infinite variance, for very displaced particles, the density distribution cannot be of Lévy type. In order to avoid the unphysical infinite variance of the diffusive particles, Shlesinger *et al.* [23] introduced the process that they called Lévy walk. The sites visited by the diffusive particle in the Lévy walk are the same as in the Lévy flight (random walk of Lévy type) but a time cost is imposed to the steps, penalizing the long steps, such that the average step time is infinite. For a Lévy walk, the variance of the particles positions is finite and grows with time as $\langle r^2, t \rangle \propto t^\gamma$, with $\gamma > 1$. As far as we know, the explicit form of the particle density distribution has never been calculated for any specific Lévy walk, and a crossover from a Lévy to a Gaussian distribution, as we go from the center to the tails, cannot be ruled out.

VI. CONCLUSION

An atomistic model for etching of a crystalline solid is proposed, and simulations were done for one-dimensional substrates, showing that the system scales according to the KPZ universality class. The imposition of periodic boundary conditions (PBC) in the simulations does not affect the scaling properties of the system, except for the fact the time $t_x = C_{t_x} L^{\alpha/\beta} = C_{t_x} L^{3/2}$ required for the correlation length to cover the substrate length L is reduced by a factor of 0.567. This means that the PBC makes the system effectively smaller by a factor of 0.68. However, the PBC changes the surface morphology. Simulations without PBC show that the fluctuations of the surface height, up to three standard deviations, satisfy an asymmetric Lévy distribution within the precision of the data, and only for fluctuations larger than three standard deviations the fluctuation statistics becomes approximately Gaussian. In contrast, simulations with PBC result in Gaussian surface height fluctuations, except for large negative fluctuations. The fact that the boundary condition may affect the short-range behavior, as manifested by the rms step size, is very surprising. Arguments are presented suggesting rms, that the asymmetry in the surface fluctuations is a necessary consequence of nonlinear terms on Δh , that are contained in the KPZ and other Langevin equations proposed to describe growth erosion, because those terms make the surface not invariant under the symmetry operation $h \rightarrow -h$.

ACKNOWLEDGMENT

This work was supported by the Conselho Nacional de Desenvolvimento Científico e Tecnológico.

- [1] Barabási and H. E. Stanley, *Fractal Concepts in Surface Growth* (Cambridge University Press, Cambridge, 1995).
- [2] P. Meakin, *Fractals, Scaling, and Growth far from Equilibrium* (Cambridge University Press, Cambridge, 1998).
- [3] Z. Toroczkai and E.D. Williams, *Phys. Today* **52**, 24 (1999).
- [4] F. Family and T. Vicsek, *J. Phys. A* **18**, L75 (1985).
- [5] S.F. Edwards and D.R. Wilkinson, *Proc. R. Soc. London, Ser. A* **381**, 17 (1982).
- [6] M. Kardar, G. Parisi, and Y. Zhang, *Phys. Rev. Lett.* **56**, 889 (1986).
- [7] M.J. Vold, *J. Colloid Sci.* **18**, 684 (1963).
- [8] D.E. Wolf and J. Villain, *Europhys. Lett.* **13**, 389 (1990).
- [9] M. Schroeder, M. Siegert, D.E. Wolf, J.D. Shore, and M. Plischke, *Europhys. Lett.* **24**, 563 (1993).
- [10] M. Siegert, *Phys. Rev. E* **53**, 3209 (1996).
- [11] G. Poupard and G. Zumofen, *J. Phys. A* **25**, L1173 (1992).
- [12] W.H. Press, S.A. Teukolsky, W.T. Vetterling, and B.P. Flannery, *Numerical Recipes in C* (Cambridge University Press, Cambridge, 1992).
- [13] J.M. López, *Phys. Rev. Lett.* **83**, 4594 (1999).
- [14] V.K. Horváth, F. Family, and T. Vicsek, *J. Phys. A* **24**, L25 (1991).
- [15] Y.-C. Zhang, *J. Phys. (France)* **51**, 2129 (1990).
- [16] J.G. Amar and F. Family, *J. Phys. A* **24**, L79 (1991).
- [17] S. Havlin, S.D.V. Buldyrev, H.E. Stanley, and G.H. Weiss, *J. Phys. A* **24**, L925 (1991).
- [18] A.S. Chaves, *Phys. Lett. A* **239**, 13 (1998).
- [19] F.A. Oliveira, B.A. Mello, and I.M. Xavier, *Phys. Rev. E* **61**, 7200 (2000).
- [20] M.F. Shlesinger, G.M. Zaslavsky, and J. Klafter, *Nature (London)* **363**, 31 (1993).
- [21] C. Tsallis, *Phys. World* **10**, 42 (1997).
- [22] A.F.G. Monte, S.W. Silva, J.M.R. Cruz, P.C. Morais, and A.S. Chaves, *Phys. Lett. A* **268**, 430 (2000).
- [23] M.F. Shlesinger, B.J. West, and J. Klafter, *Phys. Rev. Lett.* **58**, 1100 (1987).